Frontiers of Information Technology & Electronic Engineering
www.jzus.zju.edu.cn; engineering.cae.cn; www.springerlink.com
ISSN 2095-9184 (print); ISSN 2095-9230 (online)
E-mail: jzus@zju.edu.cn

Supplementary materials for

Xiaojun ZOU, Guangming WANG, Yawei WANG, Wei SONG, Hang ZHU, Ming TAN, Xuguang XU, Guoqin KANG, Binfeng ZONG, 2025. A parasitic coupling network concept for mutual coupling utilization in wideband multielement antenna arrays. *Front Inform Technol Electron Eng*, 26(4):652-670.
https://doi.org/10.1631/FITEE.2300742

1 PCN for the three-element linear array

For a 1×3 antenna array with three elements, the ARCs of both the middle and edge elements should be taken into account. Similarly, it is easy to judge whether the mutual coupling among the three-element array can be utilized or not. Fig. S1 plots the *S*-parameters, phase differences, and prototype of the original three-element H-plane antenna array. For port 1, the simulated band is 4.4–5.7 GHz (25.7%), and the mutual coupling in 3–4.54 GHz assists the ARC band to expand to 4.08–5.62 GHz (31.8%). Additionally, the measured results demonstrate an identical trend. However, due to the strong coupling from the edge elements, the impedance matching of the middle antenna is apparently worse than that of the single one. As the magnitudes related to port 2 fail to meet the demand $|S_{21}+S_{23}|\leq 2|S_{22}|$ in 4.6–4.9 GHz (plotted in Fig. S1c), the ARC of element 2 is above −10 dB, resulting in a limited shared band. Therefore, a PCN is required to ameliorate the situation and further widen the shared ARC band.

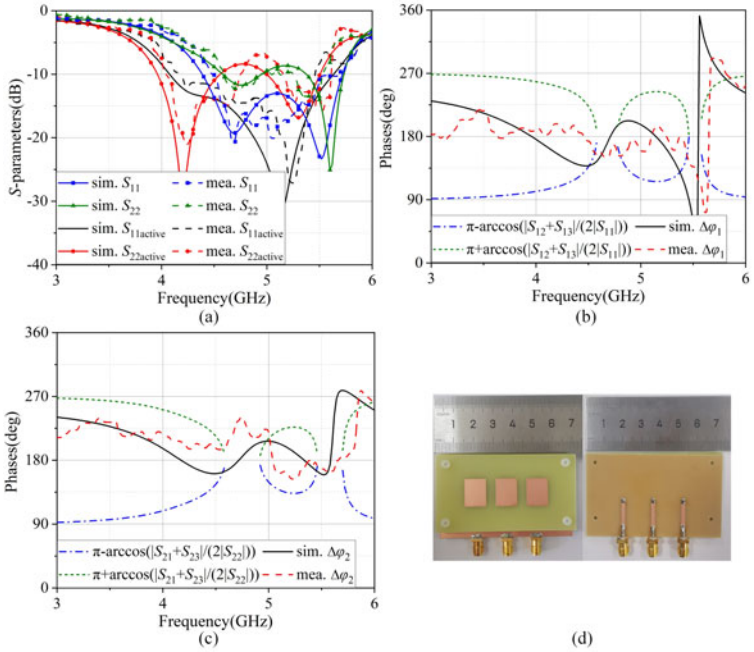

Fig. S1 *S*-parameters, phase differences, and prototype of the original three-element H-plane antenna array: (a) *S*-parameters; (b) phase difference of port 1; (c) phase difference of port 2; (d) the fabricated array

Fig. S2 exhibits the proposed PCN for the three-element H-plane antenna array. On account of the coupling environment that is different to that of the two-element one, the shunt arms of the two shorted T-stubs are unequally contrived to fully use mutual coupling. The dimensions that vary from those in Fig. 6c are: l_{h1}=5.7 mm, l_{h2}=8.5 mm, w_{h4}=3 mm, l_{h4}=9.6 mm, l_{h6}=3.7 mm, and l_{h8}=5.7 mm. Afterwards, the *S*-parameters, phase differences, and prototype of the three-element H-plane antenna array with the PCN are illustrated in Fig. S3. In almost the entire given band, which is 3.0–5.4 GHz, the mutual coupling can be employed to widen the operating band of element 1; thus, its measured ARC band is 3.88–5.86 GHz (40.7%), developing from the reflection coefficient band of 4.65–5.72 GHz (20.6%). For element 2, owing to the available coupling band of 3.68–5.04 GHz, the measured ARC band is 3.94–5.86 GHz (39.2%), stemming from the reflection coefficient band of 5.02–5.76 GHz (13.7%). Hence, the shared operating band of the antenna array with the PCN is 3.94–5.86 GHz (39.2%).

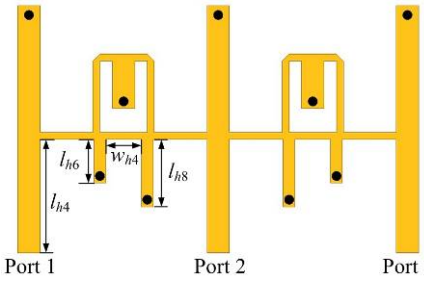

Fig. S2 The proposed PCN for the three-element H-plane antenna array

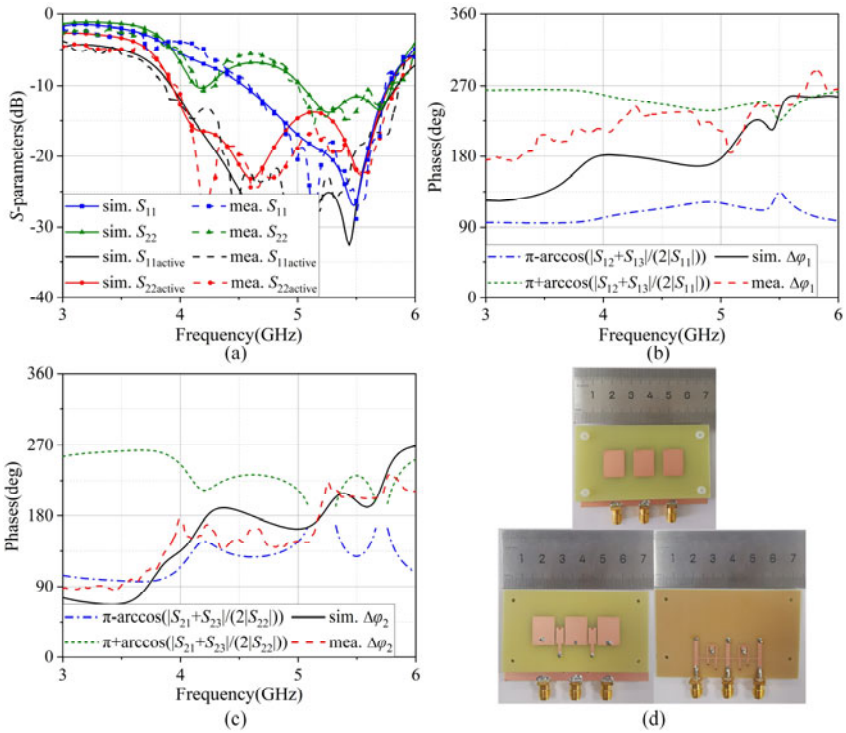

Fig. S3 *S*-parameters, phase differences, and prototype of the three-element H-plane antenna array with the PCN: (a) *S*-parameters; (b) phase difference of port 1; (c) phase difference of port 2; (d) the fabricated array

Meanwhile, the simulated and measured normalized radiation patterns, and gains and radiation efficiencies of the three-element H-plane antenna arrays without or with the PCN are plotted in Figs. S4 and S5, respectively.

It is noteworthy that the added PCN exerts influence on the backward radiation, which increases a little owing to the extra radiation of the PCN, especially in the high band, but the broadside gains in the operating band stay steady above 7.0 dBi and the cross-polarization levels in the H-plane remain low. Moreover, the simulated and measured radiation efficiencies of the antenna array with the proposed PCN are respectively over 73.5% and 71.9%, demonstrating its good radiation characteristic.

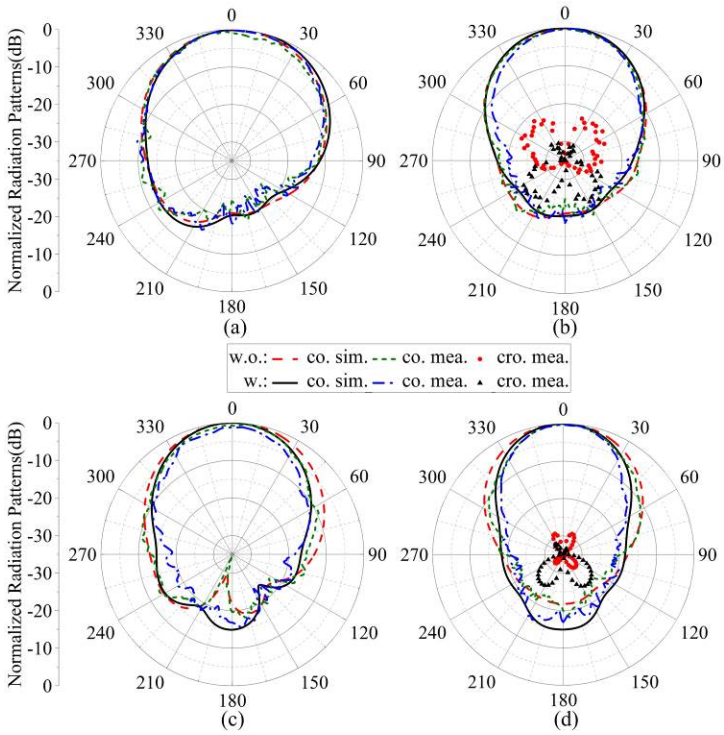

Fig. S4 Simulated and measured normalized radiation patterns of the three-element H-plane antenna array without or with the PCN: (a) E-plane and (b) H-plane at 4.1 GHz; (c) E-plane and (d) H-plane at 5.6 GHz

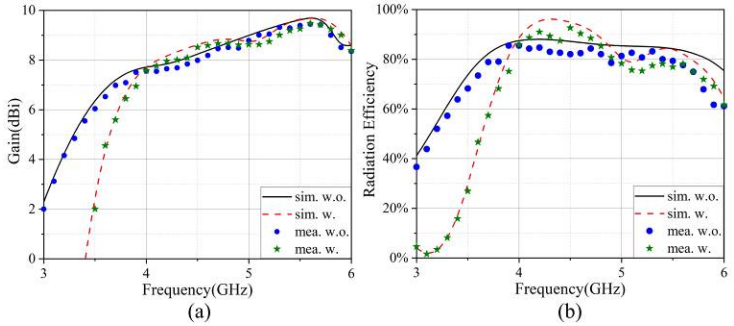

Fig. S5 Simulated and measured gains and radiation efficiencies of the three-element H-plane antenna array without or with the PCN: (a) gain; (b) radiation efficiency

2 PCN for the five-element linear array

Moreover, the PCN is further extended to a five-element 1×5 H-plane antenna array to verify its effectiveness and explore its capability in a phased array. As $M\times N$ turns to 1×5, the ARCs and coupling utilization conditions of elements 1, 2, and 3 can also be obtained according to Eq. (3) and inequality (5).

Likewise, the characteristics of the original antenna array have previously been analyzed. Fig. S6 presents the *S*-parameters, ARCs, phase differences, and prototype of the original five-element H-plane antenna array. It is apparent that the mutual coupling aids the ARCs of elements 1 and 2 to widen the bands, but not that of element 3, which suffers from the same situation of the middle element in the original three-element antenna array. In the band of 4.52–4.88 GHz, the constitutive condition is not satisfied, leading to the enlargement of the ARC; so, the shared operating band is limited.

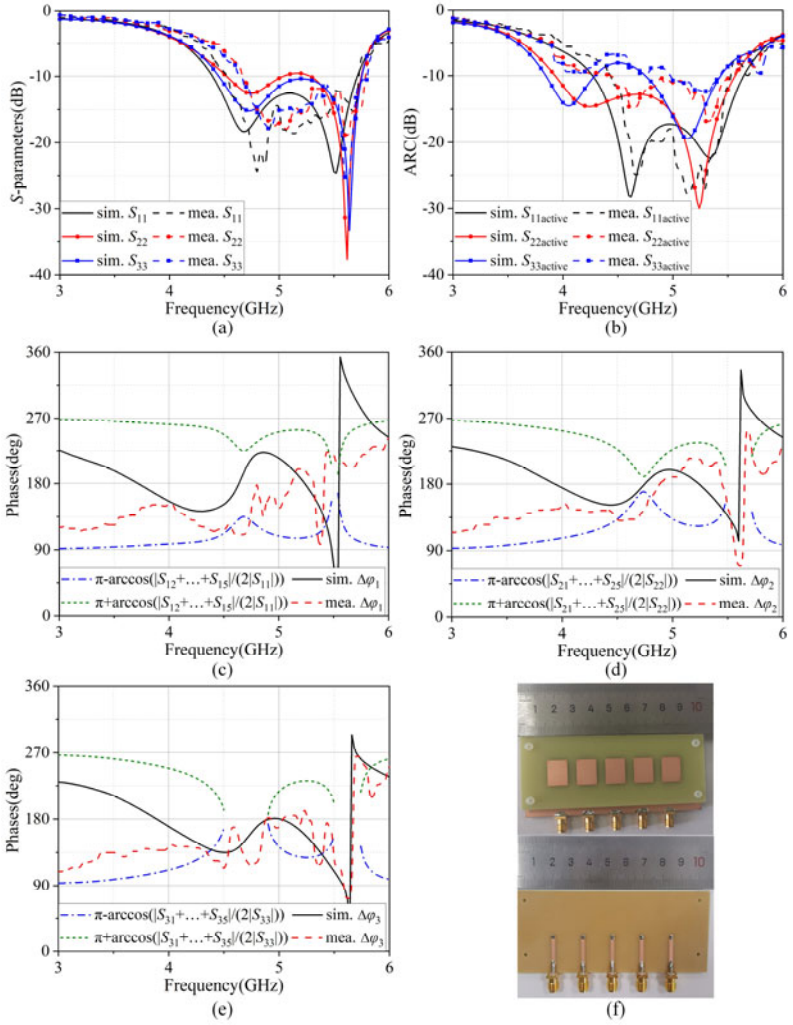

Fig. S6 *S*-parameters, ARCs, phase differences, and prototype of the original five-element H-plane antenna array: (a) *S*-parameters; (b) ARCs; (c) phase difference of port 1; (d) phase difference of port 2; (e) phase difference of port 3; (f) the fabricated array

Hence, on the basis of the PCN for the three-element array, an extended one is put forward for the five-element array, as shown in Fig. S7. To maintain the symmetry of the array, both of the parasitic elements and the coupling network are symmetrically distributed along the middle element. To make the working band as wide as possible, the parasitic elements between array elements 1 and 2, array elements 2 and 3 are finely adjusted to accommodate various coupling environments, as is the coupling network. The modified dimensions are: l_{h1}=6.2 mm, l_{h2}=5 mm, w_{h4}=3 mm, l_{h4}=7.6 mm, l_{h6}=5.7 mm, l_{h8}=3.7 mm, l_{h9}=6.2 mm, and l_{h10}=3 mm. Then, the antenna array with the novel PCN is simulated, fabricated, and measured, and the results are plotted in Fig. S8. The figure illustrates that the overlapped ARC bandwidth is greatly widened via loading the PCN. For element 1, the phase difference in Fig. S8c can account for its bandwidth improvement, as the measured curve

falls within the lower and upper boundaries in 3.46–4.82 GHz, which successfully extends S_{11} of 4.54–5.72 GHz (23%) to $S_{11\text{active}}$ of 3.52–5.76 GHz (48.3%). However, for elements 2 and 3, the situation is somewhat different in that there are deficient bands (3.82–3.9 GHz for port 2 and 3.86–3.9 GHz for port 3) missing the boundary values. Still, the mutual coupling in these bands is properly utilized to enable the ARC bandwidths to expand to 3.7–5.6 GHz (40.9%) and 3.66–5.68 GHz (43.3%) for elements 2 and 3, respectively. The shared operating band ultimately falls in 3.7–5.6 GHz (40.9%), which is a huge enhancement compared with that of the original array.

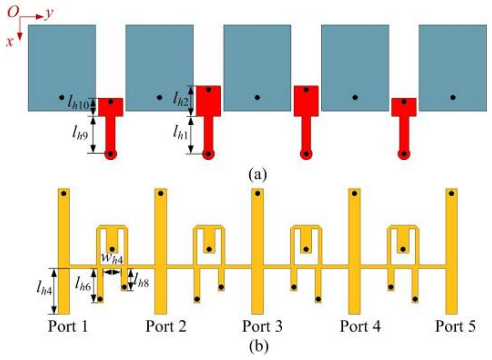

Fig. S7 The proposed PCN for the five-element H-plane antenna array: (a) parasitic elements; (b) coupling network

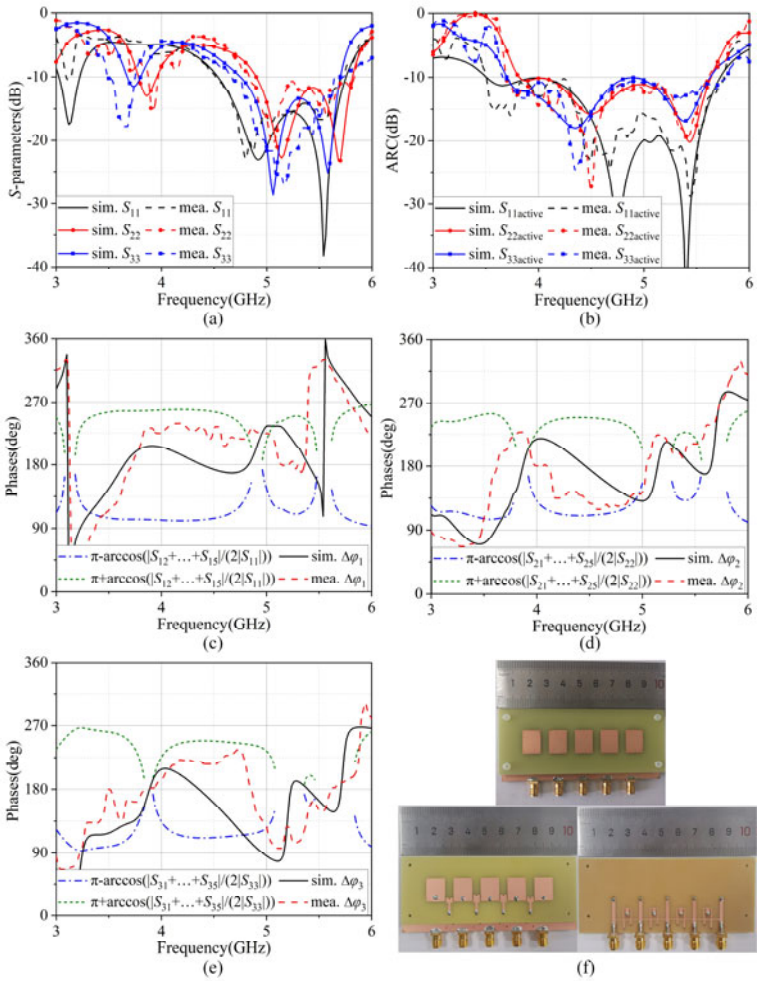

Fig. S8 *S*-parameters, ARCs, phase differences, and prototype of the five-element H-plane antenna array with the PCN: (a) *S*-parameters; (b) ARCs; (c) phase difference of port 1; (d) phase difference of port 2; (e) phase difference of port 3; (f) the fabricated array

With the increase of the element number, the scanning characteristics of the antenna array should be taken into account. According to Eq. (4) and inequality (5), the ARCs turn to

$$\begin{cases} S_{11\text{active}} = S_{11} + S_{12}\mathrm{e}^{-\mathrm{j}\psi} + S_{13}\mathrm{e}^{-\mathrm{j}2\psi} + S_{14}\mathrm{e}^{-\mathrm{j}3\psi} + S_{15}\mathrm{e}^{-\mathrm{j}4\psi} \\ S_{22\text{active}} = S_{21}\mathrm{e}^{\mathrm{j}\psi} + S_{22} + S_{23}\mathrm{e}^{-\mathrm{j}\psi} + S_{24}\mathrm{e}^{-\mathrm{j}2\psi} + S_{25}\mathrm{e}^{-\mathrm{j}3\psi} \\ S_{33\text{active}} = S_{31}\mathrm{e}^{\mathrm{j}2\psi} + S_{32}\mathrm{e}^{\mathrm{j}\psi} + S_{33} + S_{34}\mathrm{e}^{-\mathrm{j}\psi} + S_{35}\mathrm{e}^{-\mathrm{j}2\psi} \end{cases}, \tag{S1}$$

where $\psi=k(d+w_\mathrm{p})\sin\theta$, and the mutual coupling utilization condition can be obtained accordingly.

Fig. S9 depicts the scanning characteristics of the five-element H-plane antenna array with the PCN, including its ARCs and mutual coupling utilization condition. As the array geometry is symmetric, only the ARCs and phase differences are emphatically researched when the array scans to the $+y$ direction. According to the mutual coupling condition displayed in Figs. S9c–S9e, it can be concluded that the varying angles have a limited impact on the coupling utilization condition; thus, the coupling can still be employed to broaden the band. From the ARCs when the scanning angles reach 30° and 56° in Figs. S9a and S9b, the impedance matching is a little deteriorated, but the ARC is lower than −8 dB (VSWR<2.3) in the overlapped band of 3.88–5.74 GHz (38.7%), which is also an acceptable level. Fig. S10 presents the scanning patterns at 4 GHz and 5 GHz, which indicate the remaining good radiation from −55° to 55° of the antenna array with the PCN, with only 2.5 dB and 3.0 dB gain loss from the maximums of 8.8 dBi and 10.9 dBi, respectively. In addition, from the cross-polarized patterns, it is implied that the cross-polarization levels increase when the array scans to a larger angle, but are still lower than −16 dB. Thus, the PCN is also applicable to one-dimensional phased arrays. Therefore, these two examples indicate the effectiveness of the PCN for multielement linear antenna arrays.

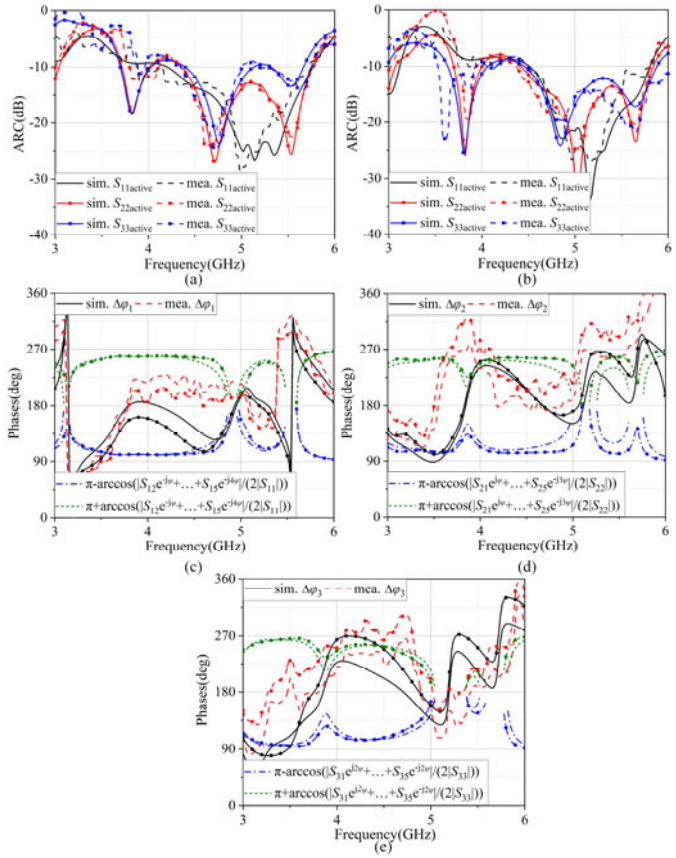

Fig. S9 Scanning characteristics of the five-element H-plane antenna array with the PCN: (a) ARC of scanning angle 30°; (b) ARC of scanning angle 56°; (c) phase difference of port 1 (line: 30°; line+symbol: 56°); (d) phase difference of port 2 (line: 30°; line+symbol: 56°); (e) phase difference of port 3 (line: 30°; line+symbol: 56°)

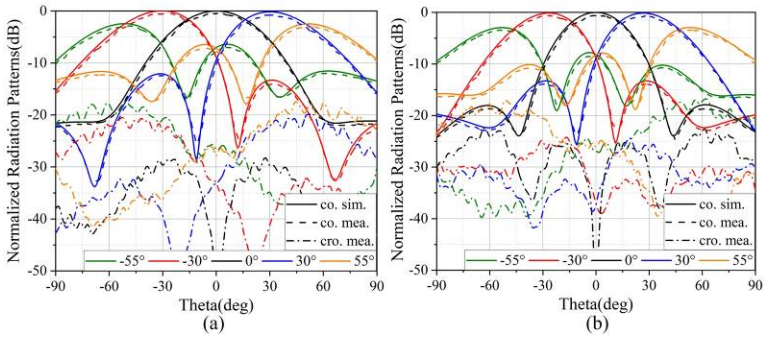

Fig. S10 Normalized scanning radiation patterns of the five-element H-plane antenna array with the PCN: (a) 4 GHz; (b) 5 GHz